T.C.
EGE ÜNİVERSİTESİ

BİLİMSEL ARAŞTIRMA PROJELERİ KOORDİNASYON BİRİMİ

PROJE BAŞLIĞI

Damla Sulama Sisteminde Suyun Toprakta Üç Boyutlu Hareketi ve Oluşan Islatma Deseninin Yeni Bir Yöntemle Matematiksel Olarak Tanımlanması

Proje No:
2016-ZRF-060

Proje Türü
Araştırma projesi

SONUÇ RAPORU

Proje Yürütücüsü:
Doç. Dr. Murat KILIÇ

Ziraat Fakültesi - Tarımsal Yapılar ve Sulama Bölümü - Tarımsal Yapılar ve Sulama Ana Bilim Dalı

Araştırmacının Adı Soyadı
Birimi/Bölümü
-

Ekim, 2018

İZMİR

Önsöz

Su kaynaklarının kentsel, endüstriyel ve tarımsal amaçlı kullanımında artan rekabet nedeniyle, tarımsal üretime ayrılan pay gittikçe azalmaktadır. Bu yönüyle damla sulama yöntemi hem üretimden sağlanan verim ve gelir artışı, hem de kıt kaynakların sürdürülebilir kullanımı açısından büyük önem taşır. Özellikle su kaynaklarının kısıtlı olduğu pek çok ülkede bu yöntem bir seçenek olmaktan çok gereklilik halini almıştır.

Damla sulama yönteminde oluşan ıslatma deseni, sistemin optimum projelenmesi ve sulamanın programlanması üzerinde doğrudan etkilidir. Bu araştırmada damla sulama sisteminde meydana gelen ıslatma deseni ve bunu oluşturan bileşenlerin koordinat sisteminde şekilsel ve boyutsal düzeyde analitik olarak tanımlanması amaçlanmıştır. Sulama uygulaması esnasında herhangi bir anda toprak profili içerisinde meydana gelen maksimum ıslatma derinliği, maksimum ıslatma genişliği, ıslak kesit alanı ve toprak yüzeyinde oluşan ıslatma yarıçapı, modelin temel bileşenlerini oluşturmaktadır. Bu parametreler zamanın bir fonksiyonu olarak düşünülmüştür. Islatma desenini tanımlayan denklemlerin elde edilmesinde, ıslak alan kesitini oluşturan bileşenler doğrudan modele dâhil edilmiştir.

Bu araştırma kapsamında gerçekleştirilen modelleme sürecinin, damla sulama uygulamalarında ıslatma deseninin tanımlanmasına yönelik temel ortak özellikleri önemli düzeyde içerdiği söylenebilir. Şöyle ki, sulama uygulamaları farklı toprak koşullarında, farklı damlatıcı debisi ile farklı sürelerde gerçekleştirilebilir. Bu değişken koşullarda oluşan ıslatma desenleri, şekilsel olarak birbirine göre daha yassı, daha şişkin, daha uzun veya daha kısa özelliklere sahip olabilir. Ancak, bunların tamamı araştırma kapsamında analitik olarak tanımlanan ortak özellikleri taşımaktadır. Sonuç olarak, damla sulama sistemi farklı özellikler gösteren ortamlarda uygulansa bile, modelin söz konusu veriler için çalıştırılması, burada oluşan ıslatma deseninin tanımlanması için yeterlidir.

Araştırmanın yürütülmesinde finansal destek sağlayan Ege Üniversitesi Bilimsel Araştırma Projeleri Koordinasyon Birimi'ne teşekkürlerimi sunarım.

Aralık, 2018

CONTENTS

Page

TABLES

Table Page

FIGURES

Figure Page

Figure Page

Özet

Damla sulama yönteminde meydana gelen ıslatma deseninin analitik olarak tanımlanması, sistemin doğru projelenmesi, sulamanın optimum programlanması ve kıt kaynakların sürdürülebilir kullanımı açısından büyük önem taşır. Islatma desenini oluşturan bileşenlerin zamansal ve mekânsal boyutta değişimi, bunların göreli hızları arasındaki ilişkilerin belirlenmesine olanak sağlar. Böylece, sulamanın başlangıcından itibaren geçen herhangi bir t_0 anında meydana gelen ıslatma deseni, zamanın bir fonksiyonu olarak ifade edilebilir. Bu süreçte, ıslatma desenini oluşturan bileşenlerin ardışık ölçümlerini güvenilir şekilde gerçekleştirmek için bir deneme tasarlanmış ve bu periyot süresince gerçek zamanlı kamera kayıtları alınmıştır. Sulama uygulaması esnasında herhangi bir anda toprak profili içerisinde meydana gelen maksimum ıslatma derinliği, maksimum ıslatma genişliği, ıslak kesit alanı ve toprak yüzeyinde oluşan ıslatma yarıçapı, modelin ve ıslatma deseninin temel bileşenlerini oluşturmaktadır. Her 5 dk'lık zaman noktasında değişkenlerin boyutları ölçülmüş ve bunlar arasındaki ilişkiler zamanın bir fonksiyonu olarak tanımlanmıştır. Bu süreçte, damla sulama uygulamasının gerçekleştirildiği toprak örneğine ait sulama yönünden önemli bazı fiziksel ve kimyasal özellikler belirlenmiştir. Ayrıca, denemenin yürütüldüğü arazide çift silindirli infiltrometre ile infiltrasyon testi yapılmıştır. Islatma desenine ilişkin denklemlerin elde edilmesinde, ıslak alan kesitini oluşturan bileşenler doğrudan modele dâhil edilmiştir. Sonraki aşamada, denemeden elde edilen ölçüm verileri ve model sonuçları karşılaştırılarak, yeni yöntemin geçerliliği analiz edilmiştir. Ulaşılan sonuçlar, tasarlanan modellerin damla sulama sisteminde ıslatma desenini oluşturan bileşenlerin göreli hızları arasındaki ilişkileri ve ıslak kesit alanını tanımladığını göstermiştir.

Anahtar kelimeler: Damla sulama sistemi, ıslatma deseni, matematiksel modelleme.

Abstract

Analytical description of the wetting pattern in drip irrigation systems is very important from the points of view of the correct projecting of the system, optimum programming of irrigation and sustainable use of deficit resources. Spatio-temporal variations of the components of the wetting pattern allow determination of the relationships between the relative rates of change of the components. Thus, the entire wetting pattern can be described as a function of time. This process allows description of the wetting pattern which occurs at any elapsed time of t_0 from the beginning of irrigation. The aim of this investigation was to determine the relationships between the relative rates of change of the components of the wetting pattern, and to describe this pattern analytically in a drip irrigation system. In this process, an experiment was designed to carry out reliable consecutive measurements of the components of the wetting pattern. Also, real-time camera records were taken during this period of time. The wetting diameter on the soil surface, the maximum wetting depth and the maximum wetting width in the soil profile are the main components of the cross-sectional area of the wetting pattern and the model. The sizes of the variables were measured at each five-minute time point. The relationships between these variables were then described as a function of time. In this process, some physical and chemical properties, important for irrigation, were determined for the soil sample on which irrigation applications were performed. Apart from this, the infiltration test was carried out by the double ring infiltrometer technique in the field where the experiment was conducted. The model devised contains directly the components of the wetting pattern. In the next stage, the data from the measurements of the experiment and the results of the models were compared. In this way, the validity of the models devised was verified. The results indicated that these models could describe the cross-sectional area of the wetting pattern and the relationships between the relative rates of change of the components of the wetting pattern in drip irrigation system.

Key words: Drip irrigation system, wetting pattern, mathematical modelling.

1. Introduction

The wetting pattern is an important factor to consider when designing and managing a drip irrigation system. The dimensions of the pattern are imperative in selecting the right spacing between emitters and a suitable distance between laterals (Al-Ogaidi et al, 2016). The movement of water in soils involves a number of physical processes. The simplest physical description of a porous medium in general, and of soils in particular, is that of a solid matrix made of grains with interconnected pores forming channels through which fluids flow (Parlange, 1974). Considering the complexity of the physical phenomena involved, the attention during the last 50 years has been focused on techniques to model the soil moisture transfer using a variety of methods. Enhanced by the advances in computers, mathematical modelling has been recently applied to various classes of problems in irrigated fields. A number of models have been developed for use in trickle systems (Ghali, 1989; Rolston et al., 1991; Angelakis et al., 1993; Colombo and Or, 2006; Wang et al., 2006). However, there remains the need for models to simulate the combined, and in some cases, simultaneous processes of water entry and multi-dimensional moisture redistribution in soil (Ghali, 1989).

In trickle irrigation, only a part of the field is wetted, typically at a high frequency. This results in complex multi-dimensional moisture transfer patterns which are influenced by field and operating conditions (Ghali, 1989; Simunek et al., 1999; Singh et al., 2006; Raine et al., 2007; Elmaloglou and Malamos, 2007; Elmaloglou and Diamantopoulos 2008; Bhatnagar and Chauhan, 2008; Souza et al., 2009; Kandelous and Simunek, 2010a; Soulis et al., 2015; Qin et al., 2016; dos Santos et al., 2016). The soil water content or soil water storage at various locations away from the trickle irrigation source will depend upon the rate of irrigation, distance from the source, water evaporation from soil surfaces, soil surface infiltration characteristics, the microtopography of the soil around the irrigation source, hydraulic characteristics of the soil, and water uptake patterns by roots (Rolston et al., 1991).

Mathematical models have been developed to simulate soil water movement considering trickle sources as point sources (Bhatnagar and Chauhan, 2008). Surface trickle irrigation involves soil water movement from a saturated disc that is formed due to water spreading on the soil surface until the infiltration rate matches the emitter discharge. The disc radius varies in time. Therefore, under a single emitter, a three-dimensional flow of water in unsaturated soil occurs from a saturated disc which has a moving boundary, i.e. the disc radius is a function of time (Brandt et al., 1971; Bhatnagar and Chauhan, 2008).

Numerical or analytical solutions of flow problems for trickle irrigation have been obtained considering a constant radius disc source. Similarly, the models developed for disc infiltrometers may also be extended to trickle irrigation. However, such models with constant disc radius are applicable only under the special conditions of long time irrigation, or soil water movement after irrigation is cut off (Bhatnagar and Chauhan, 2008). Because of its highly localized application and its flexibility in scheduling water and chemical applications, drip irrigation has gained widespread popularity as an efficient and economically viable method for fertigation (Mmolawa and Or, 2000), and there are a number of models that describe infiltration from a point or line source that can be used to design, install, and manage drip irrigation systems.

Elmaloglou and Malamos (2007) carried out an investigation of the estimation of width and depth of the wetted soil volume under a surface emitter, considering root water-uptake and evaporation. A cylindrical flow model that describes local infiltration from a surface point source was used to obtain numerical results. However, the wetting front of the emitters in the soil profile does not have an exact parabolic shape. The maximum width of the wetting front may occur under the soil surface. Under a trickle source, the flow of water in unsaturated soil takes place from a disc source with a radius which changes with time. An unsteady, nonlinearised numerical model was developed by Bhatnagar and Chauhan (2008) in an oblate spheroidal coordinate system to predict the wetting pattern below an emitter placed on the soil surface. However, relative rates of change of the components of the wetting pattern at different time points were not taken into consideration. The increased use of water of marginal quality with drip irrigation requires sound fertigation practices that reconcile environmental concerns with viable crop production objectives. Souza et al. (2009) conducted experiments to characterize the dynamics and patterns of soil solution within the wet bulb formed by drip irrigation. However, no analytical solution was developed to describe the components of the wetting pattern of drip irrigation.

Elmaloglou and Diamantopoulos (2009) investigated the infiltration and redistribution of soil moisture under surface drip irrigation considering hysteresis in two soils of different texture (loamy sand and silt loam). In this study, a cylindrical flow model incorporating hysteresis in the soil water retention characteristic curve, evaporation from the soil surface and water extraction by roots was used. However, relative rate of change and acceleration of the components of the wetted area pattern for drip irrigation were not described analytically. An artificial neural network (ANN) technology was presented by Lazarovitch et al. (2009) as

an alternative to physically-based modeling of subsurface water distribution from trickle emitters. Three options were explored to prepare input-output functional relations from a database created using a numerical model (HYDRUS-2D). However, a wetted area pattern was not described analytically by a new approach for trickle emitters. Elmaloglou et al. (2010) investigated the validity of the assumption that an irrigation event from point sources could be approximated as an infinite line source. In this process, two existing mathematical models which simulate point and line drip irrigation were used. However, relative rate of change and acceleration values of the components of the wetted area pattern in drip irrigation system were not described analytically in temporal and spatial dimensions. Kandelous and Simunek, (2010b) evaluated the accuracy of several approaches used to estimate wetting zone dimensions by comparing their predictions with field and laboratory data, including the numerical HYDRUS-2D model, the analytical Wet Up software, and selected empirical models. However, a new method was not developed to describe the wetted area pattern for drip irrigation systems. The Green-Ampt infiltration model is a simplified version of the physically based full hydrodynamic model, known as the Richards equation. The simplicity and accuracy of this model facilitates its use in many field problems, such as infiltration computation in rainfall-runoff modelling, effluent transport in groundwater modelling studies, and irrigation management studies including drainage systems. The numerous infiltration models based on the Green-Ampt approach have been widely investigated for their applicability in various scenarios of homogenous soils. FuQiang et al. (2011) developed a numerical model of two-dimensional soil water movement under surface drip irrigation conditions. The physical process of soil water movement was described by the 2D Richards equation, and the upper boundary condition was depicted by the improved moving ponded area boundary. However, the wetted area pattern in the drip irrigation system was not described analytically.

Sampathkumar et al. (2012) carried out an investigation of soil moisture distribution and root characters as influenced by deficit irrigation through a drip system in a cotton-maize cropping sequence. A field experiment was carried out by Danierhan et al. (2013) in order to investigate the effects of different emitter discharge rates under drip irrigation on soil salinity distribution and cotton yield in Northwest China. Liu et al. (2013) carried out an experiment to investigate the effects of different drip irrigation regimes on the distribution and dynamics of soil water and salt. However, the components of the wetted area pattern in a drip irrigation system were not described mathematically in these investigations.

One of the most important aspects of the planning and management of a drip irrigation system is the determination of the soil moisture patterns formed under the emitter. Elmaloglou et al. (2013) investigated the soil water dynamics under surface drip irrigation from equidistant line sources using a simulation model, which combines hysteresis in the soil water characteristic curve, evaporation from the soil surface, and water extraction by roots. On the other hand, rate of change and acceleration of the components of the wetted area pattern in a drip irrigation system were not described analytically in temporal and spatial dimensions. Badr and Abuarab (2013) carried out an investigation of soil moisture distribution patterns under surface and subsurface drip irrigation systems in sandy soil using the neutron scattering technique. Water distribution uniformity was assessed by applying the Surfer Model. However, wetted area patterns in drip irrigation systems were not described analytically in the study. Kuklik and Hoang (2014) carried out an investigation of the determination of the principal relationships influencing the distribution of moisture content in a soil profile under an emitter in point irrigation. The wetted soil volume was determined by conducting field experiments. However, the wetted area pattern in a drip irrigation system was not described analytically in this investigation.

Li et al. (2015) carried out a field experiment to reveal the soil-water flow pattern beneath a combined plastic-mulch and drip irrigation system using brackish water. The soil water flow system was characterized from the soil surface to the water table based on the observed spatio-temporal distribution of total soil-water potential, water content and electric conductivity. However, the rate of change and acceleration of the components of the wetted area pattern in the drip irrigation system were not described analytically.

Kilic (2018a) carried out an investigation in order to describe the wetting pattern analytically using a new method-simultaneous double parabola design- for soils with uniform texture. In this process, some physical and chemical properties, important for irrigation, were determined for the soil sample on which irrigation applications were performed. They were such components as PH, salinity, lime, organic matter, texture, bulk density, aggregate stability, moisture content of the soil at the beginning of the irrigation application, infiltration velocity and discharge of emitter. The infiltration test was carried out by the double ring infiltrometer technique in the field where the experiment was conducted. In this part of the investigation, the laboratory experiments and their comparative analysis were represented in the model devising process. The wetting pattern and its components were observed in real-time conditions, and they were measured at each five-minute time point during the irrigation

application. Also, real-time camera records of the wetting pattern were taken during this process. Next, the wetting pattern was described analytically on the coordinate system as shape and in dimensional level. After analyzing the accuracy of the model devising process by different solution techniques, the model application stage for the experimental data was reached.

In the second part of the investigation, the model, which describes the wetting pattern in drip irrigation system, was run for the data from the laboratory experiment (Kilic, 2018b). The equations estimate the variation of the wetting pattern both on the soil surface and in the soil profile in vertical and horizontal directions at different times. The wetting diameter on the soil surface, the maximum wetting depth and the maximum wetting width in the soil profile are the main components of the cross-sectional area of the wetting pattern and the model. It was determined that the wetting pattern in the drip irrigation could be described correctly by the simultaneous double parabola approach for different mediums. The results showed that the components of the wetting pattern could be represented as a function of time.

Al-Ogaidi et al. (2016) conducted laboratory experiments with surface drip irrigation involving two soil textures (sand and clay), two discharge rates, and two soil profiles (homogeneous and layered-textural). An empirical model was developed to estimate the vertical and horizontal advance of the wetting front at different application times. The empirical model includes estimation of the wetted radius at the soil surface and the depth of the wetting pattern as a function of application time. However, the shape of the wetted area pattern in the drip irrigation system was not described analytically in temporal and spatial dimensions. Hammami and Zayani (2016) developed an analytical approach for predicting the wetted soil volume underneath an emitter laid on the ground surface. The approach was based on (1) the Green and Ampt assumption, (2) the inference of the wetted soil depth from the radius of the humid area at the ground surface, and (3) the hypothesis that the bulb keeps a semi-elliptical shape whose diagonals are merged with the soil surface and the symmetry axis. However, the wetting front of the emitters in the soil profile does not have a semi-elliptical shape, and the maximum width of the wetting front may occur under the soil surface.

Spatio-temporal variations of the components of the wetting pattern in a drip irrigation system allow determination of the relationships between their relative rates of change. Thus, the entire wetting pattern can be described as a function of time. This allows the description of the wetting pattern which occurs at any elapsed time t_0 from the beginning of the irrigation. The aim of this investigation was to determine the relationships between the relative rates of

change of the components of the wetting pattern, and to describe this pattern analytically in a drip irrigation system. In this process, a new method, relative rates of change of variables, was used in modelling the system.

2. Materials and Methods

The investigation was carried out in three main stages. The first was to determine the wetting pattern which occurred in the soil profile in the drip irrigation system by observing it in an experiment. The second was to describe the wetting pattern mathematically by placing it on the coordinate system. The third main stage of the investigation consisted of the comparison of the model results and the real data measured in the experiment.

The first stage of the investigation was handled in two sub-categories. The first was the visual description of the wetting pattern in the soil profile for different times, and the second was the measurement of the dimensions of the components constituting the wetting pattern at set five-minute intervals. For this purpose, an experiment was designed in order to perform the consecutive reliable measurements. The soil samples were taken from an agricultural area, and physical and chemical features were analyzed in the laboratory. Separately from this, the infiltration test was performed by double-ring infiltrometer in the field from which the soil samples were taken.

In preparing the soil sample for the experiment, it was first kept until it acquired the characteristics of dry air conditions, then it was crumbled, meanwhile keeping its natural granular structure. Next, the sample was put under a specially designed glass cover (Figure 1) (Watson et al., 1995; Al-Ogaidi et al., 2016). Before supplying water from the point source to the soil, available soil moisture was determined in the laboratory. The physical and chemical features of the soil sample were as follows: pH 7.71, salinity 0.051%, lime 18.12%, organic matter 0.86%, texture clay loam, bulk density 1.30 gr/cm^3, aggregate stability 45.82%, moisture content of the soil as percentage of volume at the beginning of the experiment (Pv) 6.97%.

In the next stage, water was given to the soil surface at a discharge rate of 2.4 L/hour. The flow rate of water given to the soil was determined by the measured container method in three repetitions. In the experiment, real-time camera records were taken over a period of 125 minutes, and the dimensions of the components constituting the wetting pattern were measured every five minutes over the 125-minute period.

2.1 Description of the Models for the Wetting Pattern of the Drip Irrigation System

The components of the wetting pattern and their features were described in detail in this stage. Some sample images from the experiment are given in Figure 1.

Figure 1. Images of the samples for the temporal and spatial variation of the wetting pattern in the soil profile in the drip irrigation system.

In order to observe the temporal and spatial variations in the wetting pattern more clearly, attention was paid to ensuring a large time interval between the sample images in Figure 1. When the borders of the wetting patterns in Figure 1 were processed on a computer, the images given in Figure 2 were obtained. These describe some of the components of the wetting pattern.

Figure 2. Components of the wetting pattern in the drip irrigation system.

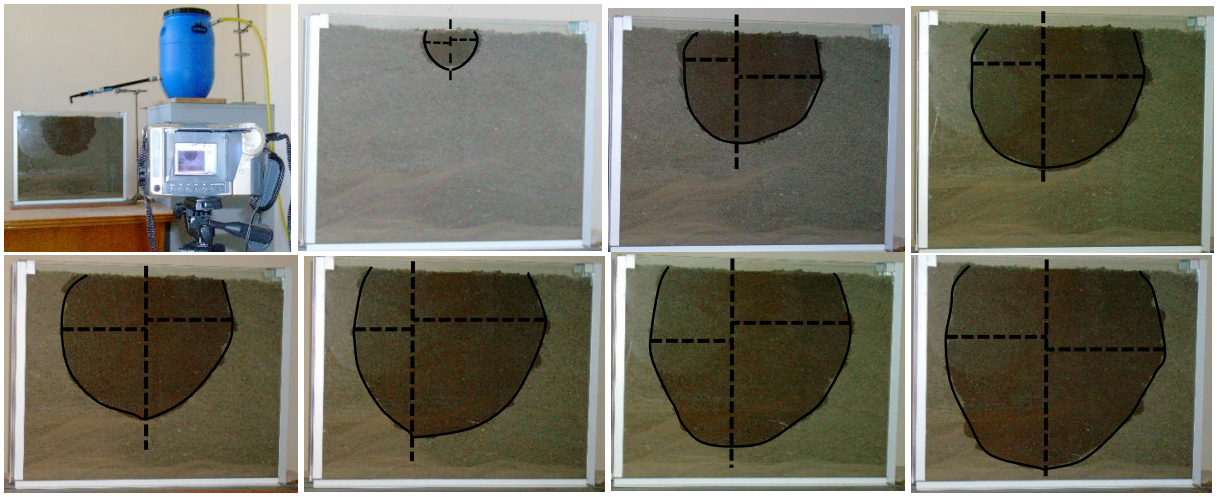

As seen in Figure 2, the maximum width of the wetting pattern occurred under the soil surface. Apart from this, the components of the wetting pattern show a continuous and

unsteady variation in temporal and spatial dimensions. These components can be considered as functions of time. The schematic view of the components of the wetting patterns is given in Figure 3.

Figure 3. Schematic view of the components of the wetting pattern in the drip irrigation system.

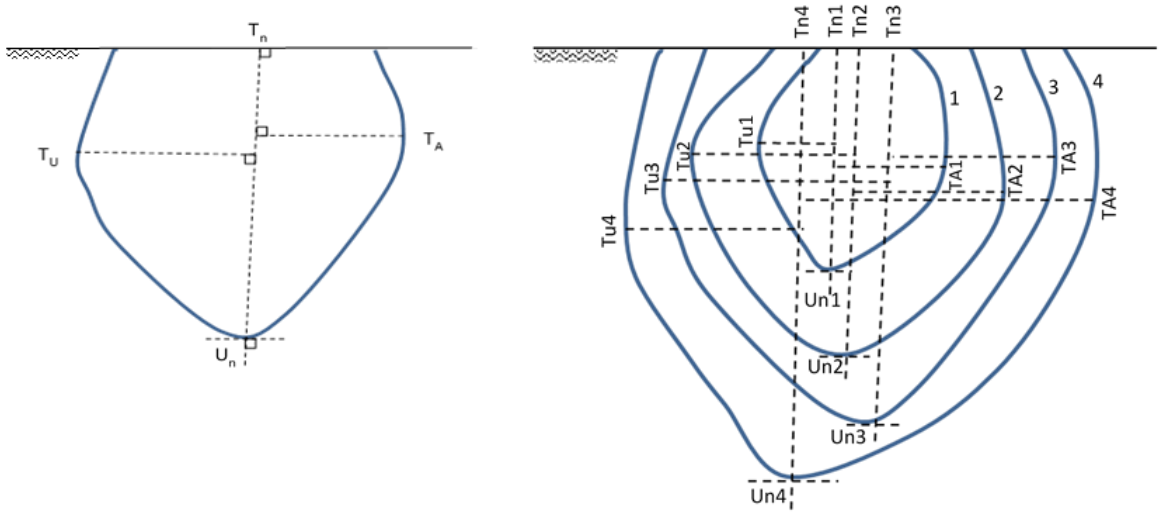

When the single wetting pattern on the left side of Figure 3 is considered

I) It is seen that the horizontal axes tangent to the points T_n and U_n are perpendicular to the line $|T_nU_n|$.

II) Line $|T_nU_n|$ shows the maximum wetting depth which occurs in the soil profile at a definite time point.

III) Points T_A and T_U, which are on the right and left sides of the line $|T_nU_n|$, are the farthest perpendicular points to this line.

IV) The line joining points T_A and T_U is perpendicular to the line $|T_nU_n|$.

On the right side of Figure 3, the wetting patterns which occurred at different time points are also shown schematically (for time points t1, t2, t3 and t4). All the cross sections of the wetting patterns determined separately for each time point are the only components simultaneously fulfilling all of the four conditions described above.

As seen in Figure 3, the maximum widths of the wetting pattern in the soil profile are represented by the symbols T_U and T_A. The components T_n, T_A, T_U and U_n of the wetting pattern show a continuous and unsteady variation in temporal and spatial dimensions. Each of them is a function of time. For instance, the line $|T_nU_n|$, perpendicular to the soil surface, and which intersects U_n, the deepest point of the wetting pattern in the soil profile, is not a symmetry axis. Also, the points T_U and T_A do not intersect each other symmetrically. During

the irrigation application, all these components showed a continuous and unsteady variation at each time point. Thus, different wetting patterns occurred both on the soil surface and in the soil profile at different time points. As seen in Figure 3, the wetting pattern occurring at each different time point joins the next one and constitutes a consecutive wetting pattern.

The second main stage of the investigation was an analytical description of the wetting pattern by placing it on the coordinate system. Turning the wetting pattern in Figure 3 90^{o} to the right makes it much easier to place it on the coordinate system. This process is shown schematically in Figure 4.

Figure 4. Placing the wetting pattern on the coordinate system in drip irrigation.

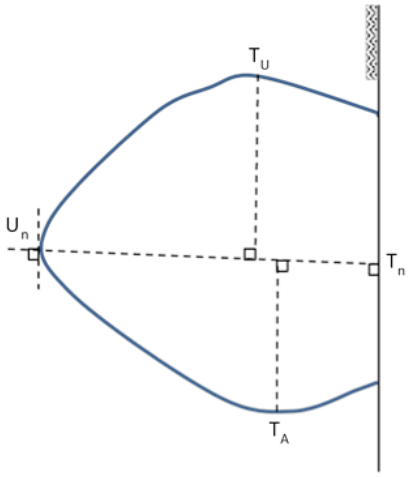

As seen in Figure 4, the line $|T_nU_n|$ represents the horizontal axis, and the soil surface constitutes the vertical axis. The area under the horizontal (X) axis was named cross section I, and that above the X axis was named cross section II. The components of cross sections I and II are completely different and independent from each other. In other words, the components of cross sections I and II do not have to be symmetric or the same size. The values of the variables constituting cross sections I and II in the wetting pattern are entered into the model separately and results are obtained. A symmetric or asymmetric wetting pattern does not change the validity of the results. As the model is run separately in accordance with the sizes of the variables constituting each of the cross sections of the wetting pattern, correct results are always obtained. This is shown schematically in Figure 5.

Figure 5. Separation of the wetting pattern in the drip irrigation into cross sections on the coordinate system.

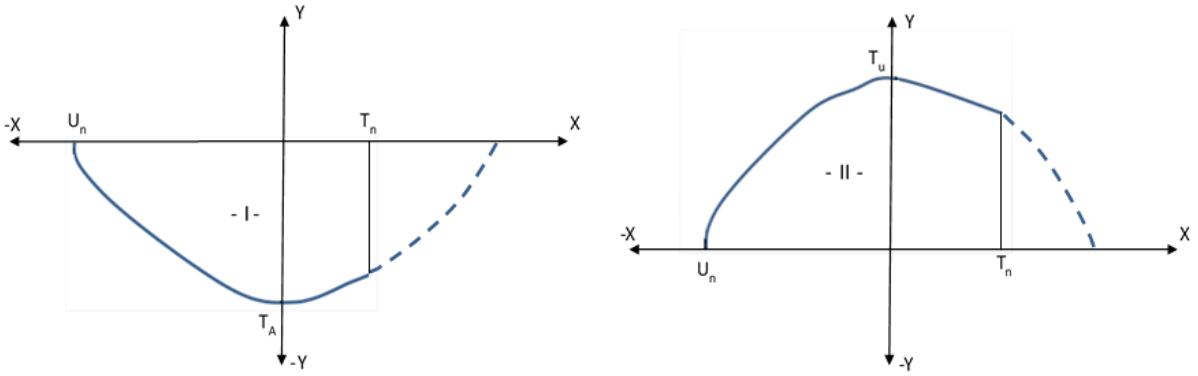

As seen in Figure 5, cross sections I and II are connected to the X axis by a dotted-line curve. Cross section I showed a convex feature, but cross section II had a concave form. As the maximum width of the wetting pattern occurs under the soil surface, cross sections I and II can perhaps be thought of as parabolas, as shown in Figure 5. The points T_A and T_U on cross sections I and II respectively can be thought of as the vertex points of the parabolas.

The components of the wetting pattern, made up of cross sections I and II, are shown schematically in Figure 6. These components were measured every five minutes during the experiment with the aim of determining the rates of change and the acceleration values of the variation of the components constituting the wetting pattern in temporal and spatial dimensions. In other words, the aim was to describe the analytic relationships between the components of the wetting pattern in a drip irrigation system.

Figure 6. Schematic description of the components of cross sections I and II constituting the wetting pattern in the drip irrigation system.

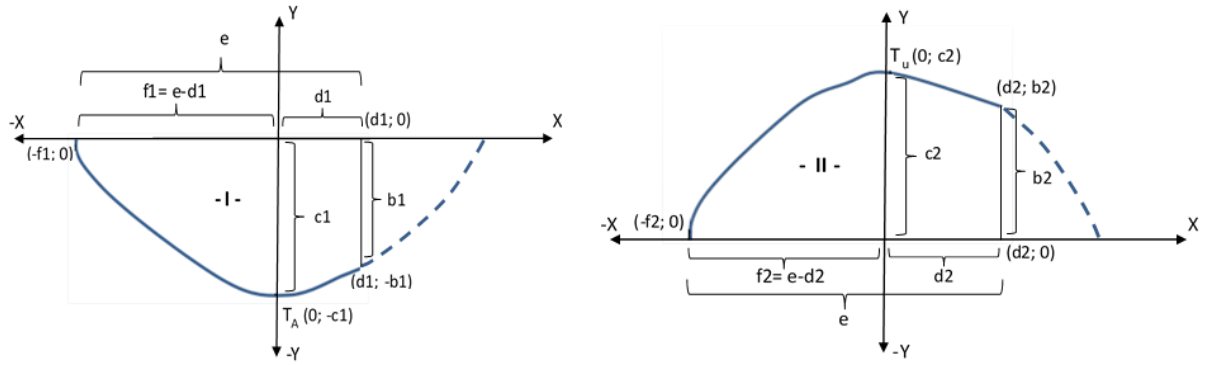

The parabola equations of the cross sections I and II (Figure 6) were represented in standard form. This equation is $y=ax^2+k$. The aim was to describe the wetting pattern more clearly and to carry out the calculation process faster and more easily.

In the equation, variation of coefficient a as the absolute value in temporal dimension determines the variation of the distance of the arms of the parabola from the y axis. In other words, increasing or decreasing absolute values of coefficient a over time indicate the arms of the parabola which constitutes the wetting pattern getting close to the y axis or moving away from it. When this was interpreted from the viewpoint of drip irrigation applications, it was seen that an increment in the amount of water infiltrating the soil or in the length of the drip irrigation period also cause an increment in the size of the wetted area occurring in the soil profile. This generally causes the arms of the parabolas constituting cross sections I and II to move away from the y axis (Figures 3 and 6). On the other hand, in this method, the $|T_nU_n|$ line, which is perpendicular to the soil surface and passes over the deepest point (U_n) of the wetting pattern, may approach or recede from the vertex points of the parabolas of cross sections I and II, depending on the location of the point U_n (Figures 3 and 5). Thus, the arms of the parabolas may get close to the y axis in some wetting patterns which occur at consecutive time points despite an increase in the total size of the wetted area, depending on the location of the line $|T_nU_n|$. The reason for this is the continuous and unsteady variation of the line $|T_nU_n|$ in the temporal and spatial dimensions. However, the total size of the wetted area also increases.

In addition, the positive or negative values of a determine the features of the parabolas as convex or concave. The term k represents the values of the ordinates of the vertex points of the parabolas which constitute cross sections I and II. As seen in Figure 6, both of the vertex points of the cross sections were located on the y axis.

The components of y, a, x and k which constitute the equation of the parabola of $y=ax^2+k$ are functions of time. This is because the wetting pattern which occurs at each different time point in the soil profile has completely different features from the previous one. That is, the sizes, rates of change and values of acceleration of the components of the wetting patterns are different from each other. In other words, these components show continuous and unsteady variations in temporal and spatial dimensions. Thus, each of them can be derived according to time. When all the components of the equation of $y=ax^2+k$ are derived according to time, the equations given below are obtained.

$$\frac{\partial y}{\partial t}=\frac{\partial a}{\partial t}x^2+2x\frac{\partial x}{\partial t}a+\frac{\partial k}{\partial t}$$

$$\frac{\partial y}{\partial t}=V_y \quad ; \quad \frac{\partial a}{\partial t}=V_a \quad ; \quad \frac{\partial x}{\partial t}=V_x \quad ; \quad \frac{\partial k}{\partial t}=V_k$$

$V_y = V_a x^2 + 2axV_x + V_k$

The vectors of rates of change providing the temporal and spatial variations of cross sections I and II, constituting the wetting pattern, are shown in Figure 7.

Figure 7. The vectors of rates of change providing the temporal and spatial variations of cross sections I and II, constituting the wetting pattern in a drip irrigation system.

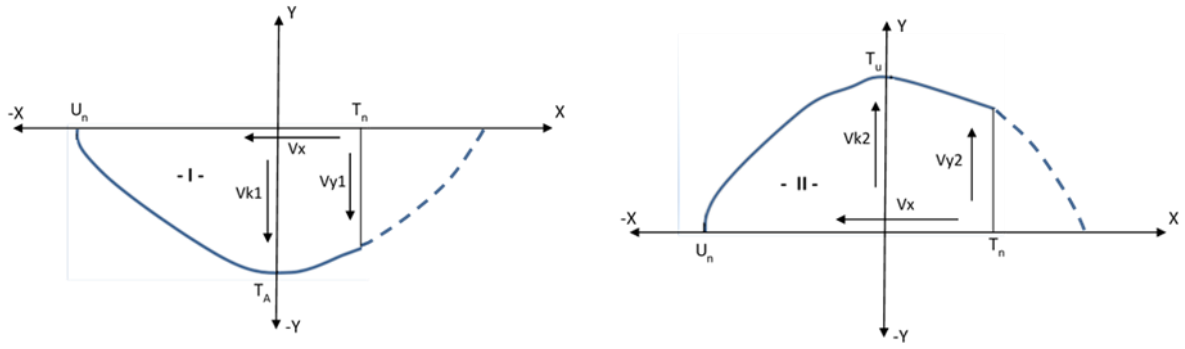

As seen in the Figure 7, the vectors V_y1 and V_y2 in cross sections I and II respectively represent the rate of change of the diameter of the wetting pattern which occurred on the soil surface. They represent the rate of change of the variables of b1 and b2 which were measured during the experiment (Figure 6). Similarly, V_k1 and V_k2 give the rate of change of the maximum width of the wetting pattern of cross sections I and II in the soil profile. They represent the rates of change of the variables c1 and c2 measured during the experiment (Figure 6). The variable V_x in the equation represents the rates of change of the variables d1 and d2, measured in cross sections I and II respectively. Similarly, the variable x in the equation also shows the lengths d1 and d2 for the cross sections I and II respectively (Figure 6). Also, the term a is the coefficient of the x^2 in the equation of the parabolas, constituting cross sections I and II. The values of a were determined separately for cross sections I and II in each time point at five minute intervals during the experiment. The term a in cross section I was obtained from the arithmetic mean of the two different values of a, which were determined according to the coordinates of (-f1;0) and (d1;-b1) shown in this cross section in Figure 6. Also, the value of the term a in cross section II was found by the arithmetic mean of the two different values of a which were obtained according to the coordinates of (-f2;0) and (d2;b2) shown in cross section II in Figure 6. In the equation, the variable V_a gives the rate of change of the coefficient of x^2 for both the parabolas in cross sections I and II. In addition, cross sections I and II, located in different zones of the coordinate system, also have different shapes from each other. While cross section I shows a convex feature, the other one has the

concave form (Figure 7). The negative or positive values of coefficient a, calculated from the equations, must describe this feature correctly. Because of this, parameter a is an indicator, determining whether or not the equations devised in this investigation are in accordance with the wetting pattern in a drip irrigation system.

In order to describe the variation of the wetting pattern in more detail in temporal and spatial dimensions in a drip irrigation system, it is very important to describe the equations of acceleration of the components of the wetting pattern. The components which show the acceleration of variation of cross sections I and II are shown schematically in Figure 8.

Figure 8. Schematic description of the components which describe the acceleration of variation of cross sections I and II, constituting the wetting pattern in a drip irrigation system.

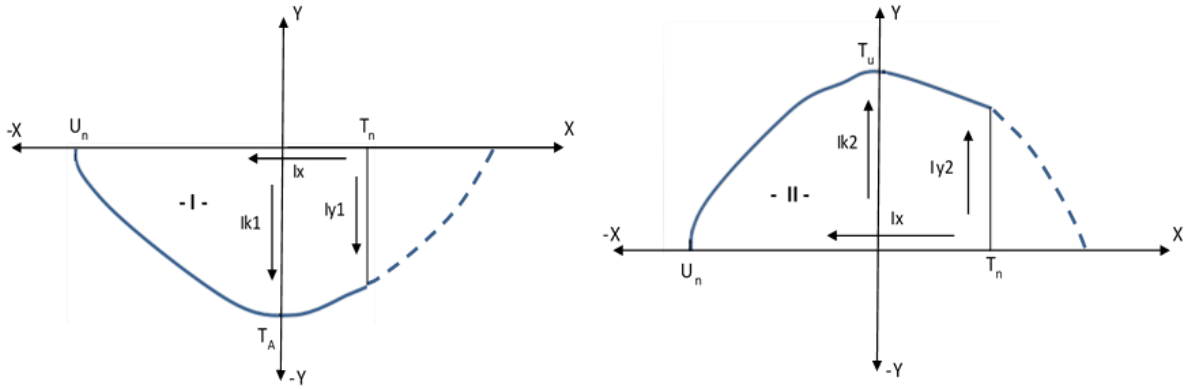

The equation of acceleration was obtained by taking the derivative of the equation of the rate of change according to the time. The processes mentioned are shown below.

$$V_y = V_a x^2 + 2axV_x + V_k$$

The derivative of the equation given above is taken according to time.

$$\frac{\partial V_y}{\partial t} = \frac{\partial V_a}{\partial t} x^2 + 2x \frac{\partial x}{\partial t} V_a + 2\left[\frac{\partial a}{\partial t} xV_x + \frac{\partial x}{\partial t} aV_x + \frac{\partial V_x}{\partial t} ax\right] + \frac{\partial V_k}{\partial t}$$

Acceleration= I

$$\frac{\partial V_y}{\partial t} = I_y \quad ; \quad \frac{\partial V_a}{\partial t} = I_a \quad ; \quad \frac{\partial V_x}{\partial t} = I_x \quad ; \quad \frac{\partial V_k}{\partial t} = I_k$$

$$I_y = I_a x^2 + 2xV_xV_a + 2[V_a xV_x + V_x aV_x + I_x ax] + I_k$$

$$I_y = I_a x^2 + 2xV_xV_a + 2xV_xV_a + 2aV_x^2 + 2I_x ax + I_k$$

$$I_y = I_a x^2 + 4xV_xV_a + 2aV_x^2 + 2I_x ax + I_k$$

This equation of acceleration was used in calculations for each five minute period when the measurements were carried out in both cross sections I and II.

2.2 Cross-Sectional Area of the Wetting Pattern

In this part of the investigation, the size of the wetted area which occurred in the soil profile was determined. In this process, the sizes of the wetted area were calculated separately for cross sections I and II, and then their sum was taken. In this way, the total size of the wetting pattern was obtained for a desired time point. For this purpose, the integral of the general equation of the parabola, described for the two cross sections, was taken. These calculation processes are given below.

$$A(T)=\int_{-x_0}^{+x_1}(ax^2+k)dx=\frac{ax^3}{3}+kx\Big]_{-x_0}^{+x_1}$$

The general equation is obtained as shown below:

$$A(T)=\frac{1}{3}ax^3+kx$$

$(-X_0;+X_1)$ are the border values in the general process, which are located on the X axis, as shown in Figure 6 for cross sections I and II. In the equation above, the values of $(-X_0;+X_1)$, which are the upper and lower borders of the integral process, represent the value of (-f1;+d1) for cross section I, and (-f2;+d2) for cross section II (Figure 6).

When determining the size of the wetted area in the soil profile in a drip irrigation system, the sum of the sizes of the areas of cross sections I and II was taken for each five minute time point when the measurements were carried out. In this way, the whole wetting pattern was described for each time point.

3. Results and Discussion

The wetting pattern constituted by cross sections I and II in the soil profile in the drip irrigation system is represented by the general equation of the parabola $y=ax^2+k$ (Figures 3 and 5). The terms a and k in the equation show the values of the coefficients of x^2 and the ordinates of the vertex points of the parabolas for cross sections I and II respectively. The values of the terms a and k, obtained at different time points for the cross sections I and II, are given in Table 1.

Table 1. The values of the terms a and k, obtained at different time points for the cross sections I and II.

Cross section I			Cross section II		
Additional time (min)	a1	k1 (cm)	Additional time (min)	a2	k2 (cm)
5	0.226	-8.5	5	-0.212	7.9
10	0.138	-9.9	10	-0.165	11.8
15	0.112	-12.9	15	-0.105	12.1
20	0.070	-14.4	20	-0.064	13.3
25	0.062	-15.8	25	-0.055	14.0
30	0.058	-16.6	30	-0.057	16.2
35	0.054	-18.5	35	-0.047	16.2
40	0.040	-18.7	40	-0.038	17.7
45	0.034	-18.9	45	-0.033	18.7
50	0.030	-19.3	50	-0.030	19.7
55	0.035	-19.9	55	-0.036	20.2
60	0.051	-20.7	60	-0.054	21.8
65	0.049	-22.3	65	-0.050	23.0
70	0.048	-23.2	70	-0.049	23.7
75	0.049	-24.1	75	-0.050	24.5
80	0.046	-24.9	80	-0.046	25.0
85	0.044	-25.4	85	-0.044	25.3
90	0.040	-26.2	90	-0.040	26.2
95	0.040	-26.5	95	-0.040	26.6
100	0.039	-27.3	100	-0.039	27.0
105	0.039	-27.5	105	-0.038	27.1
110	0.038	-28.2	110	-0.037	27.7
115	0.035	-28.3	115	-0.035	27.9
120	0.034	-28.7	120	-0.033	28.4
125	0.032	-28.9	125	-0.032	28.8

As seen in Table 1, the values of a1 and a2 obtained for cross sections I and II respectively showed a decreasing trend as absolute values over time. This shows that when the irrigation period gets longer or the amount of water infiltrating the soil increases, the wetting pattern also increases in size. In other words, the arms of the parabolas seen in Figures 3 and 5 generally showed a trend of going away from the y axis. However, a relative increment occurred in the absolute values of a1 in cross section I at the 55th, 60th and 75th minutes in relation to each previous time point. The reason is that the components of the wetting pattern show independent variations at each time point, as seen in Figures 2 and 3.

Also at the time points stated above, the arms of the parabola on the $|T_nU_n|$ axis in cross section I remained closer to the y axis than at the previous time points, as seen in Figure 5. The reason is the location of the point U_n, as shown schematically in Figure 3. The $|T_nU_n|$ axis in cross section I, shown in Figure 5, was slightly closer to T_A than its location at the previous time points in the 55th, 60th and 75th minutes. In this way, the width of the arms of the parabola at the next time point remained relatively smaller than at the previous time point. In other words, the arms of the parabola at the next time point were closer to the y axis. When the location of the $|T_nU_n|$ axis changes during the water application period, the coefficient of a will also change relatively in the equation of the parabola which occurs at each time point. A similar condition is also valid for cross section II.

The positive values of a1 in cross section I show that this parabola has a convex shape. On the other hand, the coefficients of a2 took negative values in cross section II, which shows that the parabolas constituting cross section II are concave. The coefficients of a1 and a2 obtained from the investigation took on values which were in accordance with the locations of cross sections I and II in the coordinate system (Figure 5).

The terms k1 and k2 determined for the cross sections of I and II show the ordinates of the vertex points of the parabolas given in Figure 5. The term k1 took negative values for cross section I, which was located on the negative side of the y axis. On the other hand, the term k2 took positive values for cross section II, which was in the positive side of the y axis. As seen in Table 1, the terms k1 and k2 increased as absolute values over time for both of the cross sections. The reason is that when the length of irrigation time or the amount of water infiltrating the soil increase, the wetted area in the soil profile also increases in size. This means that the parabolas which constitute the wetting patterns increase in size at each time point. Thus, as seen in Figure 5, the ordinates of the vertex points of both cross sections I and II, i.e. the values of k1 and k2, increase as absolute values, and a variation occurs in accordance with the increase in size of the wetted area.

Another subject related to the wetting pattern in the soil profile of the drip irrigation system was the estimation of the rate of change of the maximum depth of the wetting pattern at each time point in the temporal and spatial dimensions. This parameter represents the temporal variation of the length of the line $|T_nU_n|$ shown in Figure 3. As seen in Figures 3 and 5, the value of this parameter is the same for both cross sections I and II. This is because the length of the line $|T_nU_n|$ on the horizontal axis of X is equal for each of the cross sections. For instance, as seen in Figure 6, the maximum depth of the wetting pattern which formed at any

time point for cross section I was shown by the symbol e. In the equation of the parabola which constitutes cross section I, one of the values of x (root) obtained for the value of zero of y at any time point must be equal to x=-f1 or close to this value. In this way, e=d1+|f1|. The momentary and average rates of change and acceleration of variation of the maximum depth of the wetting pattern as calculated by the formula devised and as measured in the experiment are given graphically in Figure 9. The statistical comparison of the data from the experiment and the results from the model solutions was carried out by means of the formula given below (Willmott et al., 2012; Al-Ogaidi et al., 2016).

$$R^2 = 1 - \frac{\sum_{i=1}^{N}(p_i - O_i)^2}{\sum_{i=1}^{N}(O_i - M)^2}$$

In the equation, R^2 is the determination coefficient. N is the total number of pieces of data, P and O refer to the predicted and observed data respectively, while M is the mean value of the observed data.

Figure 9. The momentary and average rates of change and acceleration of variation of the maximum depths of the wetting pattern as calculated by the formulas devised and as measured in the experiment.

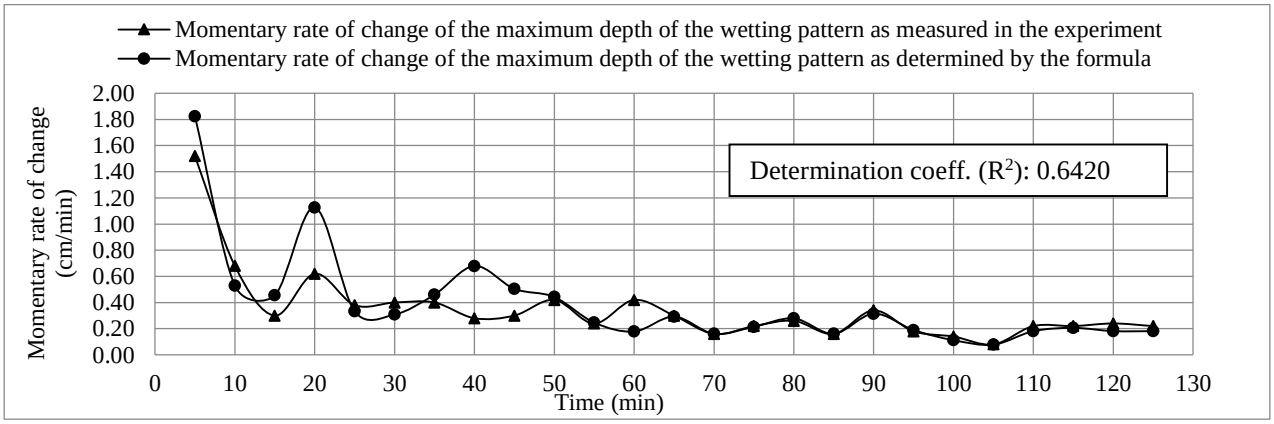

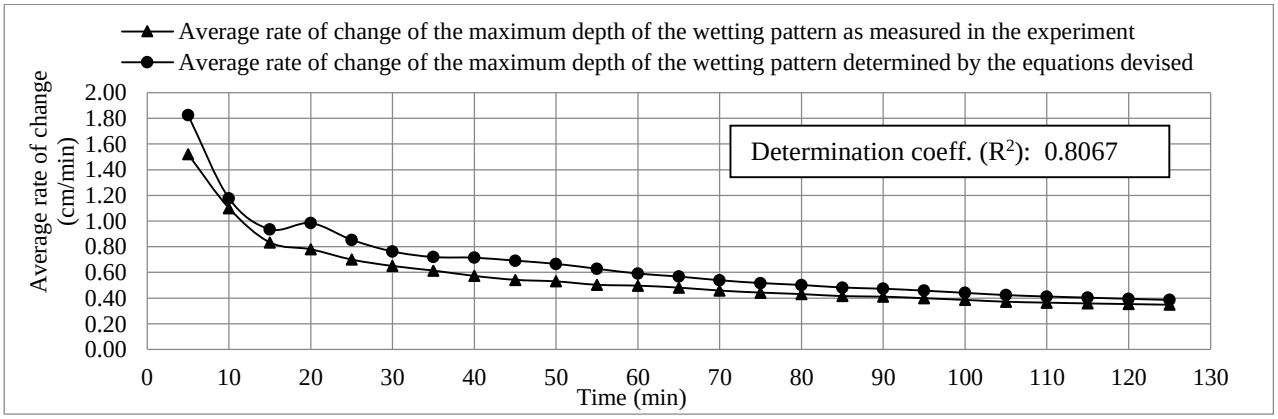

Figure 9. (Continue)

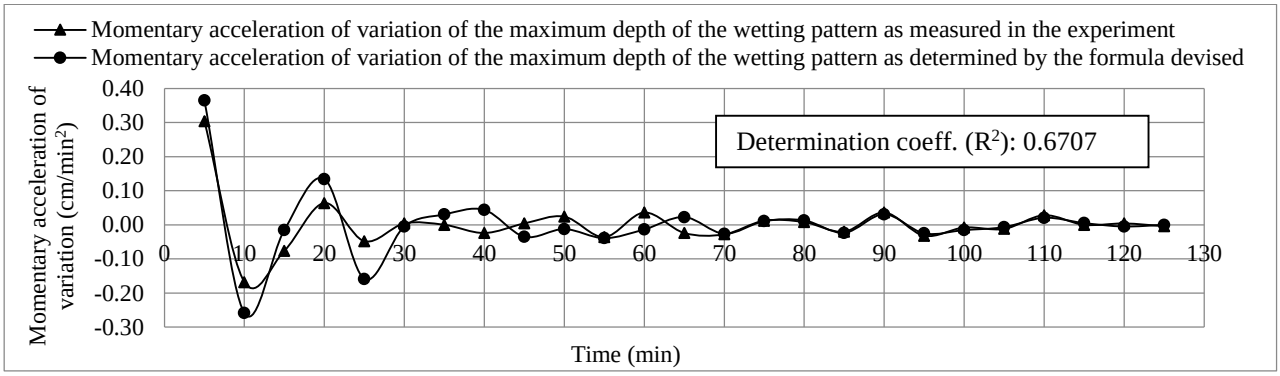

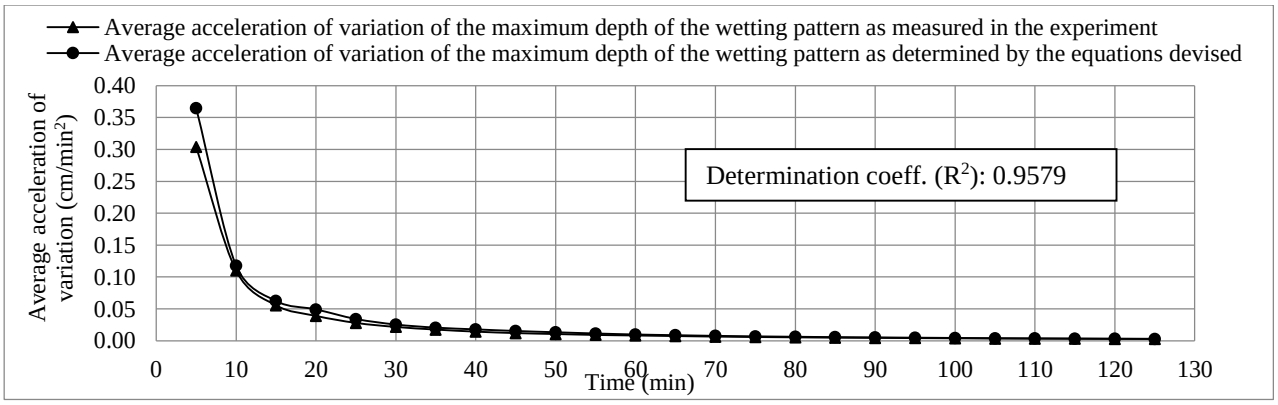

In the next main stage of the investigation, the temporal variation of the wetting diameter which occurred on the soil surface was investigated. In this process, a comparison was made of the total rate of change of the wetting diameter (V_y1+V_y2), which was calculated separately by the formulas devised for cross sections I and II respectively, and the rate of change of the wetting diameter (Vay), which was measured as a whole in the experiment. These vectors of the rate of change are given schematically in Figure 10.

Figure 10. Schematic view of the rate of change (V_y1 and V_y2) of the wetting diameter b1 and b2 which was calculated separately by the formulas devised for cross sections I and II respectively, and the rate of change (Vay) of the wetting diameter ay which was measured as a whole in the experiment.

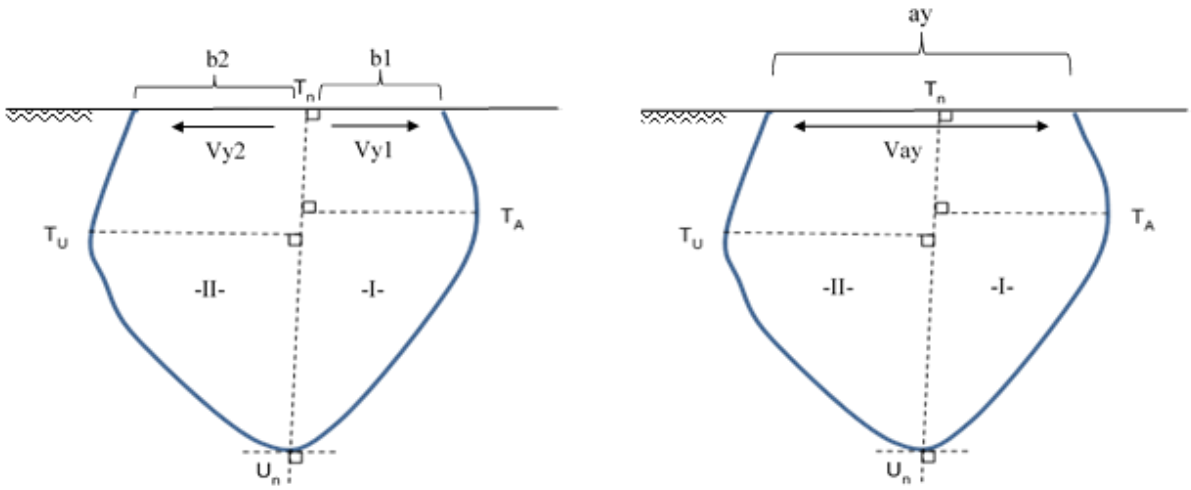

In other words, the value of (V_y1+V_y2) which was calculated by the formulas devised was compared with the temporal rate of change (Vay) of the wetting diameter (ay) on the soil surface which was measured in the experiment. These data are shown graphically below.

Figure 11. The comparison between the momentary and average values of (V_y1+V_y2); (Vay) and (I_y1+I_y2); (Iay) as calculated by the formulas devised and as measured in the experiment.

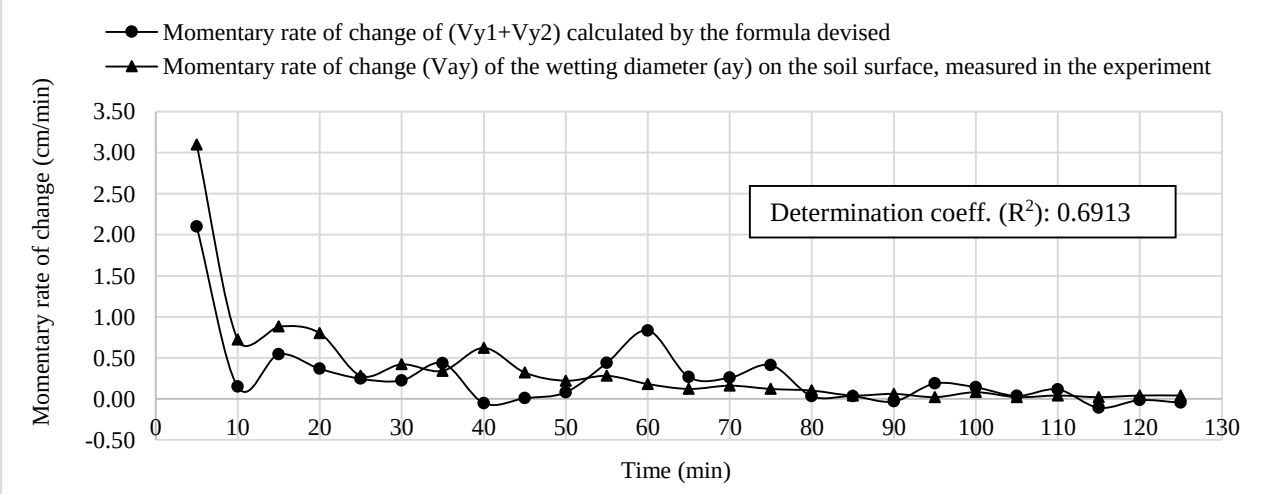

Figure 11. (continue)

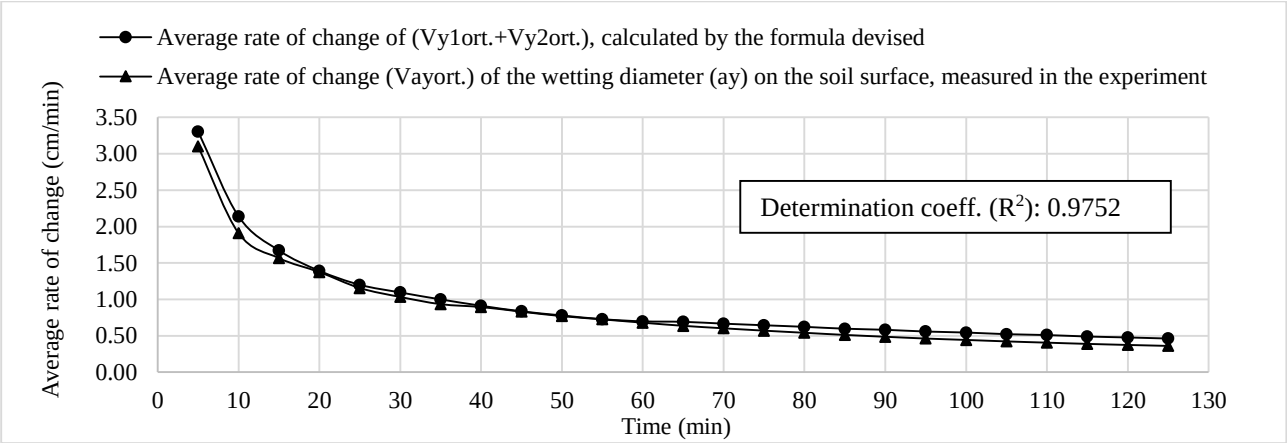

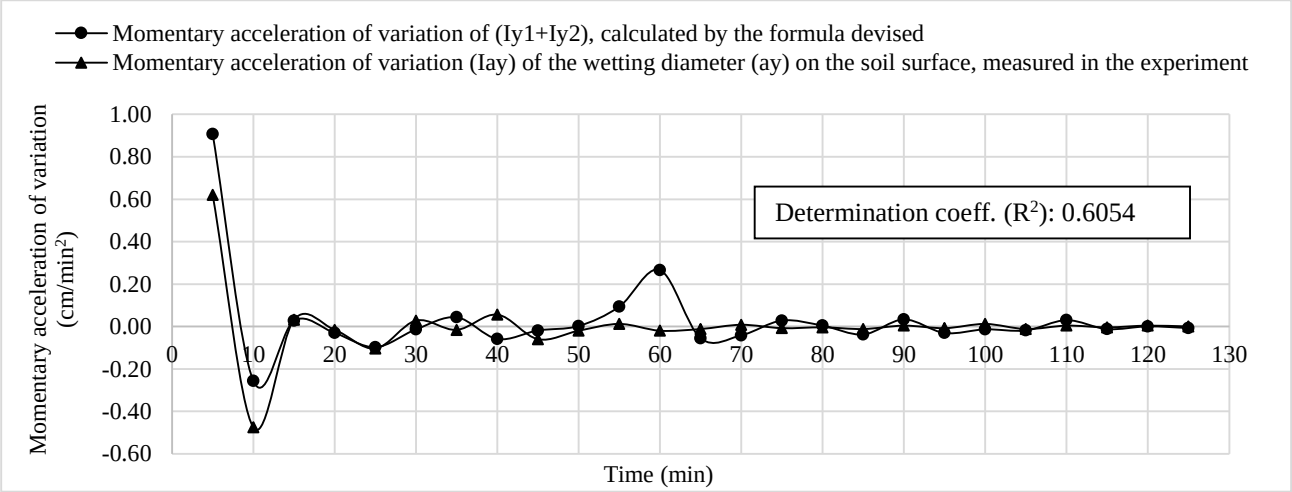

Another subject in this investigation was to research the size of the wetting pattern in the soil profile and its rate of change over time in a drip irrigation system. In this process, the sizes of the wetted areas of cross sections I and II constituting the wetting pattern were determined separately, and then the size of the wetted area which occurred in the soil profile was obtained by summing these two values for each time point. The temporal rates of change of the size of the wetted area which occurred in the soil profile for each time point when the measurements were carried out in the experiment are shown graphically.

Figure 12. The size of the wetted area in the soil profile and its temporal variation in a drip irrigation system.

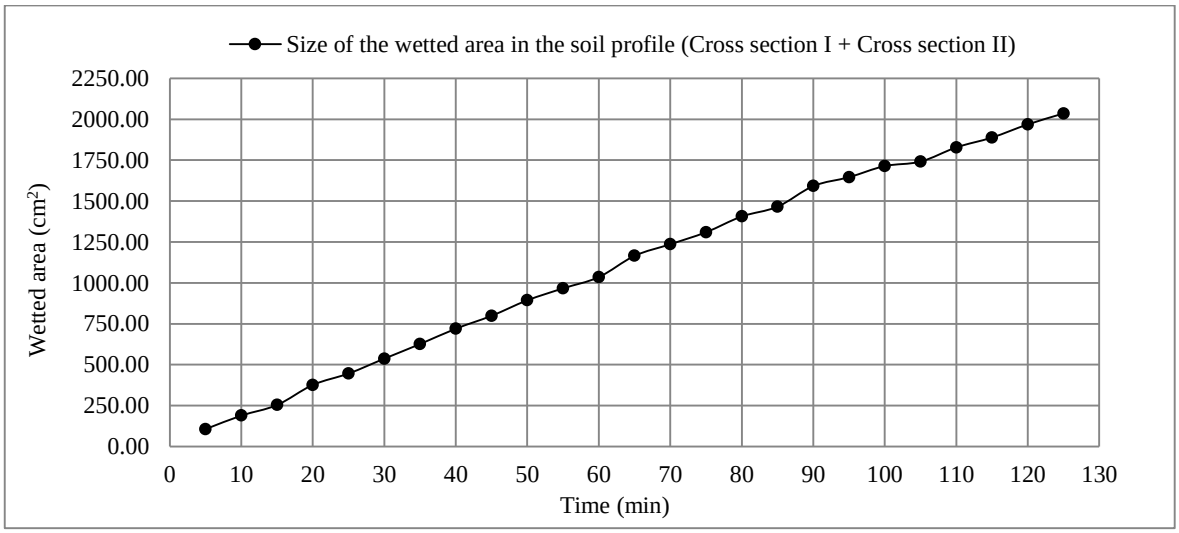

As seen in Figure 12, the size of the wetted area in the soil profile took increasing values for each time point. This shows that as the amount of water infiltrating the soil or the length of irrigation time increases, the size of the wetted area which occurs in the soil profile also increases.

As explained in the Method section, the location and length of the axis $|T_nU_n|$, the position of the vertex points T_A and T_U relative to each other, and the sizes of the wetted areas of cross sections I and II showed a continuous and unsteady variation independent of each other (Figure 3) at each time point when the measurements were carried out. However, the total size of the wetted area increased at each consecutive time point. These results show that the values of the measurements obtained from the experiment and the results from the equations devised are in accordance with each other.

The temporal rate of change of the size of the wetted area in the soil profile is shown graphically below. Both the values of the momentary and the average rates of change provided an opportunity to investigate the acceleration of variation of the size of the wetted area.

Figure 13. The momentary and average rates of change and acceleration of the variation in the size of the wetted area in the soil profile in the drip irrigation system.

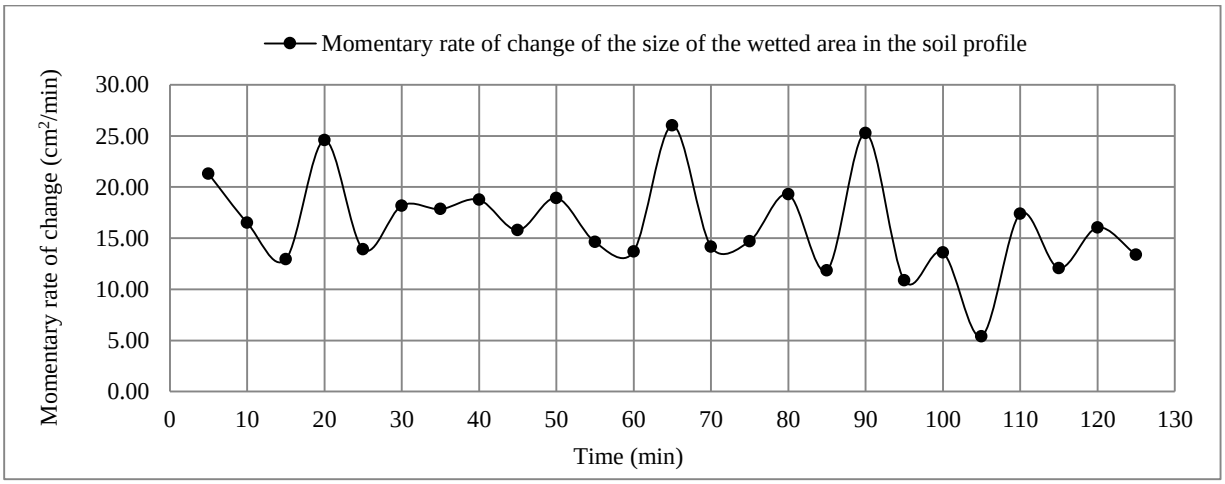

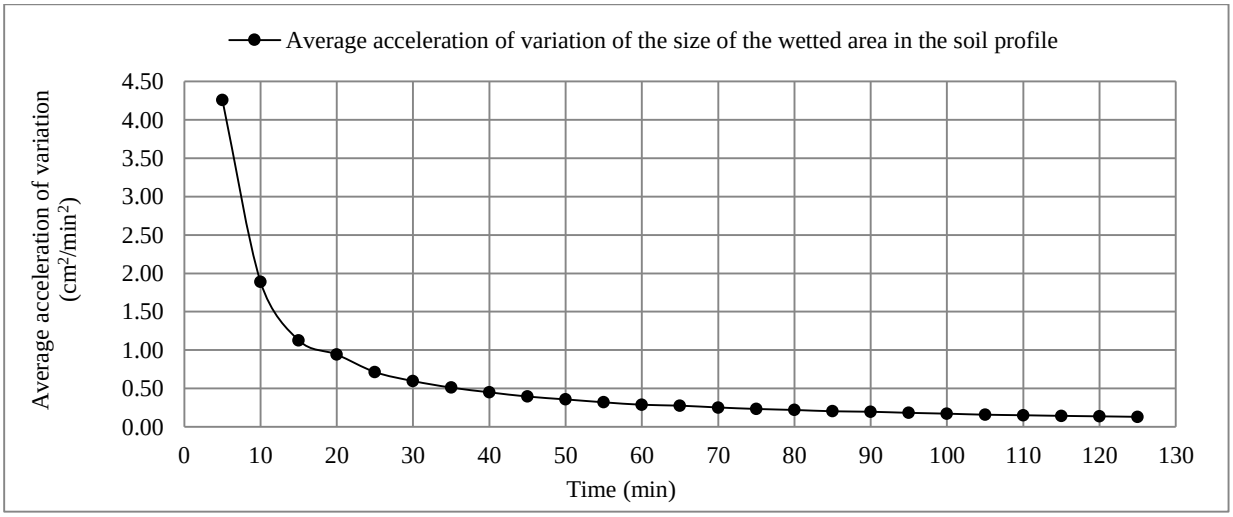

4. Conclusions

Analytical description of the rates of change of the components of the wetting pattern in a drip irrigation system in spatio-temporal dimensions is very important. The wetting pattern can be configured as a function of time. In this investigation, the wetting pattern which occurred in the soil profile was placed in the coordinate system and separated into two zones, cross sections I and II (Figures 3, 4, 5). Each cross section showed a feature in accordance with the equation $y=ax^2+k$ of the parabola. The coefficients a calculated by the formulas devised took positive values for cross section I, and negative values for cross section II (Table 1). This indicated that cross section I was convex and cross section II concave. These results showed that the models devised in this investigation represent the wetting pattern of a drip irrigation system which occurred in the soil profile.

Apart from this, coefficient a in the equation of the parabola generally took decreasing values over time as absolute values for the cross sections I and II (Table 1). This shows that the arms of the parabola which constitutes the wetting pattern go away from the y axis. In other words, as the amount of water infiltrating the soil increased or the irrigation period lengthened, the wetted area in the soil profile also increased in size. In this way, the arms of the parabolas which constituted the wetting pattern went away from the y axis depending on this enlargement (Figure 3, Figure 5). As a result, the models devised in this investigation represent the wetting pattern which occurs in the soil profile and its variation in temporal and spatial dimensions.

Relationships were found between the momentary and average rates of change and the acceleration of variation of the components of the wetting pattern as calculated by the formula devised and as measured in the experiment (Figure 9, Figure 11). These findings show that the wetting pattern can be described as a function of time.

In addition, another subject in this investigation was to determine the size of the wetted area which occurred in the soil profile at different time points, its rate of change and the values of acceleration of variation. Although the wetting pattern was separated into two zones, cross sections I and II, for each time point, the total wetted area increased in size at each consecutive time point (Figure 12, Figure 13). These results show that the measurements which were carried out in the experiment and the results from the model solutions were in accordance with each other.

When the irrigation medium, soil texture and/or emitter discharge changes, the size of the wetting pattern varies. However, the method and the equations devised in this investigation are constant, and they represent the general wetting pattern of the drip irrigation system. As a result, reliable results are obtained when the model is run for the current values of the variables. Also, this solution method can be applied widely to different investigations on this subject.

5. The meanings of the symbols used in this project

a: The coefficient of x^2 in the equations of the parabolas constituting cross sections I and II. The fact that the coefficient of a takes decreasing values as absolute values over time show that the arms of the parabolas go away from the y axis. Apart from this, while the positive values of a provide a parabola showing a convex feature, the negative values of a represent a concave parabola. The values of this parameter are an

important indicator, determining whether the model devised in this investigation represents the wetting pattern in drip irrigation.

k: Ordinate values of c1 and c2 of the vertex points T_A and T_U of the parabolas, constituting cross sections I and II respectively (cm) (Figure 5 and Figure 6).

x: The lengths of d1 and d2 which are in cross sections I and II respectively (cm) (Figure 6).

V_a: The rate of change of a which is the coefficient of x^2 in the parabolas of cross sections I and II (cm/min). In other words, this variable gives the rate of change of the distance of the arms of the parabolas in cross sections I and II from the y axis (Figures 5 and 7).

V_k: This variable represents the rate of change of the maximum width of the wetting pattern (c1 and c2) in the soil profile for cross sections I and II respectively (cm/min) (Figures 6 and 7). In other words, this variable represents the rate of change of the ordinates of the vertex points (T_A and T_U) of the parabolas, constituting cross sections I and II respectively.

V_x: The rate of change of the lengths of d1 and d2 for cross sections I and II respectively (cm/min) (Figures 6 and 7).

V_y: The rate of change of the wetted diameter (b1 and b2) on the soil surface for cross sections I and II respectively (cm/min) (Figures 6 and 7).

I_a: The acceleration of variation of a, which is the coefficient of x^2 in the equation of the parabola for cross sections I and II (cm/min^2). In other words, the acceleration of variation of the distance of the arms of the parabolas from the y axis for the cross sections I and II, which constitutes the wetting pattern in the soil profile (Figure 5).

I_k: The acceleration of variation of the maximum width of the wetting pattern (c1 and c2) in the soil profile for cross sections I and II respectively (cm/min^2) (Figures 6 and 8). In other words, acceleration of variation of the values of the ordinates of the vertex points (T_A and T_U) of the parabolas constituting cross sections I and II.

I_x: The acceleration of variation of the lengths of d1 and d2 for cross sections I and II respectively (cm/min^2) (Figures 6 and 8).

I_y: The acceleration of variation of the wetted diameter (b1 and b2) on the soil surface for cross sections I and II respectively (cm/min^2) (Figures 6 and 8).

A(T): Each size of the wetted area of cross sections I and II (cm^2), (Figures 5 and 6).

6. References

Al-Ogaidi, A.M.A., Wayayok, A., Rowshon, M.K., Abdullah, A.F., 2016. Wetting patterns estimation under drip irrigation systems using an enhanced empirical model. Agricultural Water Management 176: 203–213.

Angelakis, A.N., Kadir, T.N., Rolston, D.E., 1993. Time-dependent soil-water distribution under a circular trickle source. Water Resources Management 7: 225-235.

Badr, A.E., Abuarab, M.E., 2013. Soil moisture distribution patterns under surface and subsurface drip irrigation systems in sandy soil using neutron scattering technique. Irrig Sci 31:317–332. DOI 10.1007/s00271-011-0306-0

Bhatnagar, P.R., Chauhan, H.S., 2008. Soil water movement under a single surface trickle source. Agricultural Water Management 95; 799-808.

Brandt, A., Bresler, E., Diner, N., Ben-Asher, I., Hiller, J., Goldberg, D., 1971. Infiltration from a trickle source I. Mathematical model. Soil Sci. Soc. Am. J. 35, 675–682.

Colombo, A., Or, D., 2006. Plant water accessibility function: A design and management tool for trickle irrigation. Agricultural Water Management 82; 45–62.

Danierhan, S., Shalamu, A., Tumaerbai, H., Guan, D.H., 2013. Effects of emitter discharge rates on soil salinity distribution and cotton (Gossypium hirsutum L.) yield under drip irrigation with plastic mulch in an arid region of Northwest China. J Arid Land 5(1): 51−59. jal.xjegi.com; www.springer.com/40333. doi: 10.1007/s40333-013-0141-7

dos Santos, L.N.S., Matsura, E.E., Concalves, I.Z., Barbosa, E.A.A., Nazário, A.A., Tuta, N.F., Elaiuy, M.C.L., Feitosa, D.R.C., de Sousa, A.C.M., 2016. Water storage in the soil profile under subsurface drip irrigation: Evaluating two installation depths of emitters and two water qualities. Agricultural Water Management 170; 91–98.

Elmaloglou, S., Diamantopoulos, E., 2008. The effect of hysteresis on three-dimensional transient water flow during surface trickle irrigation. Irrigation and Drainage 57(1); 57-70.

Elmaloglou, S., Diamantopoulos, E., 2009. (Short communication) Effects of hysteresis on redistribution of soil moisture and deep percolation at continuous and pulse drip irrigation. Agricultural Water Management 96; 533-538.

Elmaloglou, S., Diamantopoulos, E., Dercas, N., 2010. Comparing soil moisture under trickle irrigation modeled as a point and line source. Agricultural Water Management 97; 426–432.

Elmaloglou, S., Soulis, K.X., Dercas, N., 2013. Simulation of soil water dynamics under surface drip irrigation from equidistant line sources. Water Resour Manage 27:4131–4148. DOI 10.1007/s11269-013-0399-8

Elmaloglou, S.T., Malamos, N., 2007. Estimation of width and depth of the wetted soil volume under a surface emitter, considering root water-uptake and evaporation. Water Resour Manage 21:1325–1340. DOI 10.1007/s11269-006-9084-5

FuQiang, T., Long, G., HePing, H., 2011. A two-dimensional Richards equation solver based on CVODE for variably saturated soil water movement. Science China. Technological Sciences. Vol.54, No.12: 3251–3264. doi: 10.1007/s11431-011-4566-y

Ghali, G.S., 1989. Multi-dimensional analysis of soil moisture dynamics in trickle irrigated fields. I: Mathematical modelling. Water Resources Management 3; 11-34.

Hammami, M., Zayani, K., 2016. An analytical approach to predict the moistened bulb volume beneath a surface point source. Agricultural Water Management 166; 123–129.

Kandelous, M.M., Simunek, J., 2010a. Numerical simulations of water movement in a subsurface drip irrigation system under field and laboratory conditions using HYDRUS-2D. Agricultural Water Management 97; 1070–1076.

Kandelous, M.M., Simunek, J., 2010b. Comparison of numerical, analytical, and empirical models to estimate wetting patterns for surface and subsurface drip irrigation. Irrig Sci 28:435–444. DOI 10.1007/s00271-009-0205-9

Kilic, M., 2018a. Analytical description of the wetting pattern in a drip irrigation system by a new method, simultaneous double parabola design. I: Method. 1st International Congress on Agricultural Structures and Irrigation. Antalya, Turkey. (In press).

Kilic, M., 2018b. Analytical description of the wetting pattern in a drip irrigation system by a new method, simultaneous double parabola design. II: Application. 1st International Congress on Agricultural Structures and Irrigation. Antalya, Turkey. (In press).

Kuklik, V., Hoang, T.D., 2014. Soil moisture regimes under point irrigation. Agricultural Water Management 134; 42– 49.

Lazarovitch, N., Poulton, M., Furman, A., Warrick, A.W., 2009. Water distribution under trickle irrigation predicted using artificial neural networks. J Eng Math 64:207–218. DOI 10.1007/s10665-009-9282-2

Li, X., Shi, H., Simunek, J., Gong, X., Peng, Z., 2015. Modeling soil water dynamics in a drip‐irrigated intercropping field under plastic mulch. Irrig Sci 33:289–302. DOI 10.1007/s00271-015-0466-4

Liu, M., Yang, J., Li, X., Liu, G., Yu, M., Wang, J., 2013. Distribution and dynamics of soil water and salt under different drip irrigation regimes in northwest China. Irrig Sci 31:675–688. DOI 10.1007/s00271-012-0343-3

Mmolawa, K., Or, D., 2000. Root zone solute dynamics under drip irrigation: A review. Plant and Soil 222: 163–190.

Parlange, J.Y., 1974. Water movement in soils. Geophysical Surveys 1: 357-387. D. Reidel Publishing Company, Dordrecht-Holland.

Qin, S., Li, S., Kang, S., Du, T., Tong, L., Ding, R., 2016. Can the drip irrigation under film mulch reduce crop evapotranspiration and save water under the sufficient irrigation condition? Agricultural Water Management 177; 128–137.

Raine, S.R., Meyer, W.S., Rassam, D.W., Hutson, J.L., Cook, F.J., 2007. Soil–water and solute movement under precision irrigation: knowledge gaps for managing sustainable root zones. Irrig Sci 26:91–100. DOI 10.1007/s00271-007-0075-y

Rolston, D.E., Biggar, J.W., Nightingale, H.I., 1991. Temporal persistence of spatial soil-water patterns under trickle irrigation. Irrig Sci 12:181-186.

Sampathkumar, T., Pandian, B.J., Mahimairaja, S., 2012. Soil moisture distribution and root characters as influenced by deficit irrigation through drip system in cotton–maize cropping sequence. Agricultural Water Management 103: 43– 53

Simunek, J., Sejna, M., van Genuchten, M.Th., 1999. The Hydrus-2d software package for simulating the two-dimensional movement of water, heat and multiple solutes in variably-saturated media, Version 2.0. Rep IGWMC-TPS-53, Int. Ground Water Model. Cent., Colorado School of Mines, Golden.

Singh, D.K., Rajput, T.B.S., Singh, D.K., Sikarwar, H.S., Sahoo, R.N., Ahmad, T., 2006. Simulation of soil wetting pattern with subsurface drip irrigation from line source. Agricultural Water Management 83; 130-134.

Soulis, K.X., Elmaloglou, S., Dercas, N., 2015. Investigating the effects of soil moisture sensors positioning and accuracy on soil moisture based drip irrigation scheduling systems. Agricultural Water Management 148; 258–268.

Souza, C.F., Folegatti, M.V., Or, D., 2009. Distribution and storage characterization of soil solution for drip irrigation. Irrig Sci 27:277–288. DOI 10.1007/s00271-008-0143-y

Wang, F.X., Kang, Y., Liu, S.P., 2006. Effects of drip irrigation frequency on soil wetting pattern and potato growth in North China Plain. Agricultural Water Management 79; 248–264.

Watson, J., Hardy, L., Cordell, T., Cordell, S., Minch, E., Pachek, C., 1995. Subject: How Water Moves Through Soil, https://tr.scribd.com/document/80543003/az9516 , (August, 2018)

Willmott, C.J., Robeson, S.M., Matsuura, K., 2012. A refined index of model performance. Int. J. Climatol. 32, 2088-2094